RSC Advances

PAPER

View Article Online
View Journal | View Issue

Cite this: *RSC Adv.*, 2020, **10**, 11300

Cellulose-based self-healing hydrogel through boronic ester bonds with excellent biocompatibility and conductivity†

Heng An,[a] Yunyi Bo,[b] Danyang Chen,[a] Yong Wang,[c] Haijun Wang,[a] Yingna He*[b] and Jianglei Qin *[ac]

Self-healing hydrogels based on degradable resources have developed rapidly in the past decade due to their extensive bioapplications with biosecurity. In this research, a new kind of cellulose-based self-healing hydrogel with bio-degradability is constructed through boronic ester linkage. The carboxyethyl cellulose-*graft*-phenylboronic acid (CMC–$B(OH)_2$) was synthesized through condensation reaction conveniently and then hydrogels were prepared with dynamic boronic ester cross-linking. The chemical structures, microscopic morphologies, mechanical and self-healing properties of the hydrogels were investigated intensively through Fourier transform infrared (FT-IR) spectroscopy, rheological, SEM and tensile testing. The hydrogels formed instantly without any additional catalyst and exhibit excellent self-healing ability with good mechanical properties. Moreover, the hydrogels were applied for controlled release of doxorubicin (DOX·HCl) and showed a successive slow release profile. Importantly, the hydrogel exhibited excellent biocompatibility and show potential applications in controlled drug delivery, 3D cell culture and tissue engineering.

Received 20th December 2019
Accepted 10th March 2020

DOI: 10.1039/c9ra10736c

rsc.li/rsc-advances

1. Introduction

Inspired by the self-repairing ability of living creatures that are capable of healing damage to tissues, like skin, muscles and bones, self-healing hydrogels have developed rapidly and have made considerable progress in recent years.[1–10] Although most covalent bonds cannot reform automatically to endow self-healing ability, scientists have made great efforts to fabricate self-healing hydrogels based on a variety of dynamic covalent bonds and intermolecular force. The hydrogels could undergo fast self-healing based on noncovalent bonds like host–guest interaction,[11–15] H-bond,[16,17] and polyion complexation.[18–21] However, the hydrogels based on dynamic covalent bonds can always endow the hydrogels with self-healing properties and improved stability at the same time. The disulfide bond with reversible redox properties was used to prepare self-healing hydrogels.[22] The oxime bond as dynamic cross-linking was also investigated.[23] The imine bond based self-healing hydrogel drew great attentions because the amino-group is widely existed in chitosan.[24–26] The acylhydrazone bond was used to design large amount of self-healing hydrogels with biosafety, since the acylhydrazide group could be easily transformed form ester bond.[27–31] The boronic ester bond, which is formed from phenylboronic acid and hydroxyl groups, could also be used to design a variety of self-healing hydrogels.[32–38] Moreover, the boronic ester bond based hydrogel always show fast self-healing based on fast boronic ester exchange.

Although large amount of self-healing hydrogels showed good bio-compatibility based on biotoxicity experiment, the hydrogels based on bioresource including cellulose,[28,39,40] chitosan,[24–26,41] sodium alginate[34] and hyaluronic acid,[42,43] *etc.*[44] were more preferred since they can degrade in natural environment and ensure long term biosafety. Pettignano coupled the phenylboronic acid onto sodium alginate and prepared self-healing hydrogel through regulation of the pH.[34] However, although the boronic ester containing hydrogel was constructed from sodium alginate, the gelation and pH sensitive range prevented it from potential bioapplications. As a result, the hydrogels formed without additional triggers show more practical application potentials. In this research, phenylboronic acid group was attached onto cellulose through amido bond to prepare boronic acid functionalized cellulose (CMC–$B(OH)_2$), and then self-healing hydrogels were prepared based on six-member ringed boronic ester structure at neutral condition. The rheology behavior, self-healing property and drug release process of the self-healing hydrogels were investigated intensively. Results

[a]College of Chemistry and Environmental Science, Hebei University, Baoding City, Hebei Province 071002, China. E-mail: qinhbu@iccas.ac.cn

[b]Hebei Key Laboratory of Chinese Medicine Research on Cardio-Cerebrovascular Disease, Pharmaceutical College, Hebei University of Chinese Medicine, Shijiazhuang City, Hebei Province 050200, China

[c]Key Laboratory of Pathogenesis Mechanism and Control of Inflammatory-Autoimmune Diseases in Hebei Province, Hebei University, Baoding City, Hebei Province 071002, China

† Electronic supplementary information (ESI) available. See DOI: 10.1039/c9ra10736c

showed the hydrogel formed with various weight ratios of CMC–$B(OH)_2$ to PVA in neutral conditions and the mechanical properties could be then regulated. Compared to cellulose enhanced boronic ester based self-healing hydrogels, this hydrogel could be degraded with degradation of the cellulose backbone.[45] Also, biotoxicity experiment of CCK-8 essay and fluorescence microscope observation showed the hydrogels are biocompatible. With biodegradable cellulose component, this biodegradable self-healing hydrogel could have great potential application in bioscience like tissue engineering, drug and cell delivery vehicles, cell culture scaffolds, *etc.*

2. Experimental section

Materials

Carboxymethyl cellulose sodium (CP = 800–1200) was purchased from Sinopharm Co Ltd (Shanghai, China). 1-Ethyl-3-(3-dimethylaminopropyl)carbodiimide·HCl (EDC·HCl) was purchased from Maya Chemical Ltd (Jiaxing, China). PVA-124, 2-(*N*-morpholino)ethanesulfonic acid monohydrate (MES, 99%), *N*-hydroxysuccinimide (NHS, 96%) and 3-aminophenylboronic acid hydrochloride was purchased from Macklin Inc. (Shanghai, China). Other solvents and chemical reagents used in this research were analytical pure supplied by Kernel Chem. and used as received.

Synthesis of phenylboronic acid-modified carboxymethyl cellulose (CMC–$B(OH)_2$)

CMC–$B(OH)_2$ was prepared by coupling 3-aminophenylboronic acid onto carboxymethyl cellulose in water solution catalyzed by NHS in presence of EDC·HCl following a previously reported procedure.[28,34] First, CMC (3 g, ~12.5 mmol repeating unit) was dissolved in deionized water (97 mL) to form a 3% clear solution in a 250 mL flask, then 3-aminophenylboronic acid (1.95 g, 12.5 mmol), EDC·HCl (4.8 g, 25 mmol) and NHS (165.4 mg, 1.48 mmol) were added. The pH of the solution was regulated to 6.5 by MES and the coupling reaction was performed for 24 h at room temperature. The product was precipitated in methanol and washed twice. Then the solid product was further purified by dialysis against water for 48 h to remove unreacted 3-aminophenylboronic acid and other impurities. The CMC–$B(OH)_2$ was obtained as light brown powder after lyophilization. The successful grafting of phenylboronic acid was confirmed by ^{1}H NMR, UV absorbance and FT-IR and the grafting ratio was calculated based on peak areas of ^{1}H NMR.

Preparation of cellulose based hydrogels from CMC–$B(OH)_2$ and PVA

The boronic ester containing hydrogels were prepared by following procedure. First, CMC–$B(OH)_2$ and PVA were dissolved in deionized water respectively to obtain homogeneous solutions with final concentration of 2% (w/w). Then the two solutions were mixed together in vials with various weight ratios and vortexed into homogeneous. Then the solution was filled into corresponding moulds to form the hydrogels for various characterizations.

The rheology study of the CMC–$B(OH)_2$ based hydrogels were carried out on an AR2000ex rheometer at 25 °C. The frequency of the scan was ranged from 0.1 rad s^{-1} to 100 rad s^{-1} between a pair of 25 mm parallel plates, and the gaps were fixed to 1 mm for all experiments. The strain scan of the hydrogels was performed with increasing strain at 1 rad s^{-1} until the breakage of the hydrogels. The strain scan at different strains of 1% and 300% alternatively were also performed to track the self-healing process.

The heart shaped hydrogel plate was cut into two halves and put together in original mold with close contact. The hydrogel plate was subjected to gravity and stretched from both sides to confirm the self-healing result after 12 h. The self-healing process of the hydrogel was also observed under microscope.

In vitro biotoxicity and controlled DOX release of the hydrogel

The cytotoxicity of the hydrogel was evaluated by CCK-8 assay according to literature, the toxicity of the hydrogel diluents to CT-26 colon cancer cells was assessed by CCK-8 cell counting kit (Sigma-Aldrich).[46] The experiment was carried out as follows, mouse colon cancer (CT-26) cells were seeded in 96-well plates with 5000 per well, then the cells were cultured in RPMI-1640 medium supplemented with 10% fetal bovine serum (FBS) and 100 U mL^{-1} penicillin–streptomycin (Gibco, Shanghai China). The hydrogel solutions with various concentrations (0.001, 0.01, 0.1 and 1 mg mL^{-1}) were then added and treated for 24 h or 48 h. After that, the medium were removed and CCK-8 regent (10% v/v) was added to each well and incubated for 4 h at 37 °C. The cell viability was measured by an enzyme-linked immunosorbent assay reader (Bio-Rad 680, USA) at 450 nm. Each concentration was repeated three times and the mean value was used to define cell viability.

The toxicity of the hydrogel solution was also determined by *in vitro* fluorescence imaging. First the CT-26 cells were cultured and then the culture medium was change to hydrogel medium solution (0.2%). After cultured for 24 h or 48 h, the cells were treated by Triton and then stained by phalloidin and 4′,6-diamidino-2-phenylindole (DAPI) respectively. The morphology of the cells was observed under an inverted fluorescence microscope.

Characterizations

The ^{1}H NMR spectra of the CMC and CMC–$B(OH)_2$ were characterized on Bruker AVANCE III 600 MHz spectrometer (Bruker, Germany), the characterizations were performed in D_2O at room temperature. The FT-IR characterization was carried out on a Varian 600-IR FT-IR spectrophotometer (Varian, America). The UNICO/UV-2000 UV-Vis spectrophotometer was used to characterize the UV spectra of the CMC–$B(OH)_2$. The rheological properties of the hydrogels were determined on a TA AR2000ex rheometer (TA instrument, USA) at 25 °C, the characterization was carried out between one pair of 25 mm parallel plates. The frequency scan and strain scan were examined to determine the mechanical property of the hydrogels. The hydrogels were observed under a JSM-7500 field emission SEM (JEOL, Japan) to

characterize the morphology, the lyophilized hydrogels were broken in liquid N_2 and coated with Au for observation.

3. Results and discussions

Synthesis of CMC–B(OH)$_2$ through coupling reaction

The CMC and 3-aminophenylboronic acid were used to synthesize CMC–B(OH)$_2$ through carbodiimide coupling reaction.[34] The structure of the CMC and CMC–B(OH)$_2$ were characterized by ^{1}H NMR and FT-IR absorbance, as shown in Fig. 1. The characteristic peaks of phenylboronic acid are illustrated at 7.5 ppm after coupling reaction, along with the protons on CMC from 4.7 ppm to 3.0 ppm (Fig. 1a). The substitution degree (DS) of CMC (defined as the molar ratio of phenylboronic acid unit to the CMC unit) was calculated by comparing the integration values of the phenyl group and that of CMC. The DS was calculated to be 26% in this research, comparable to boronic acid-modified alginate.[34] The structure of the CMC–B(OH)$_2$ was also characterized by FT-IR, but the peak 1450 cm^{-1} associated to the C–B vibration was not very confirmative because of overlapping. However, the carbonyl group at 1590 cm^{-1} divided into two peaks, the new shoulder at 1670 represented the amido bond formed through coupling reaction (Fig. 1b). This proved the carboxyl group had reacted with 3-aminophenylboronic acid partially and the phenylboronic acid functional groups have been attached onto the CMC backbone. Based on UV absorbance of the phenylboronic acid, the UV characterization of CMC–B(OH)$_2$ was also carried out to confirm the coupling reaction. The absorbance of the CMC–B(OH)$_2$ showed characteristic peak at 243 nm and the absorbance increased with increasing concentrations (Fig. S1†), which also proved the phenylboronic acid had been attached onto the CMC. The decomposition temperature increased because the phenylboronic acid was attached onto the CMC and made the decomposition product hard to evaporate under heating (Fig. S2†).

Preparation of the boronic ester containing hydrogels and morphology

The hydrogels with dynamic boronic ester bond were prepared by simply mixing aqueous solutions of CMC–B(OH)$_2$ and PVA at room temperature. It was noticed the hydrogels formed almost instantly after mixing of the two solutions without any additional stimulus no matter the total concentration of 2% or 1%. The mechanism of the hydrogel formation is also shown in Scheme 1, and the optical photographs of solution (2%) and

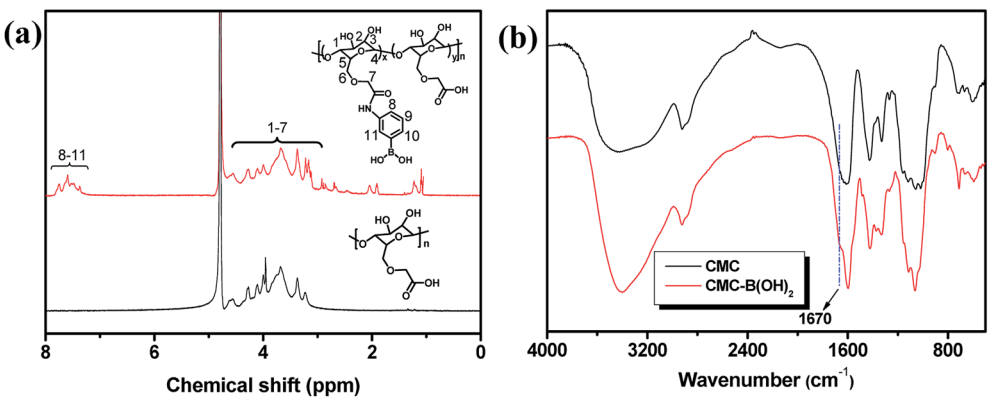

Fig. 1 ^{1}H NMR (a) and FT-IR spectra (b) of the CMC and CMC–B(OH)$_2$.

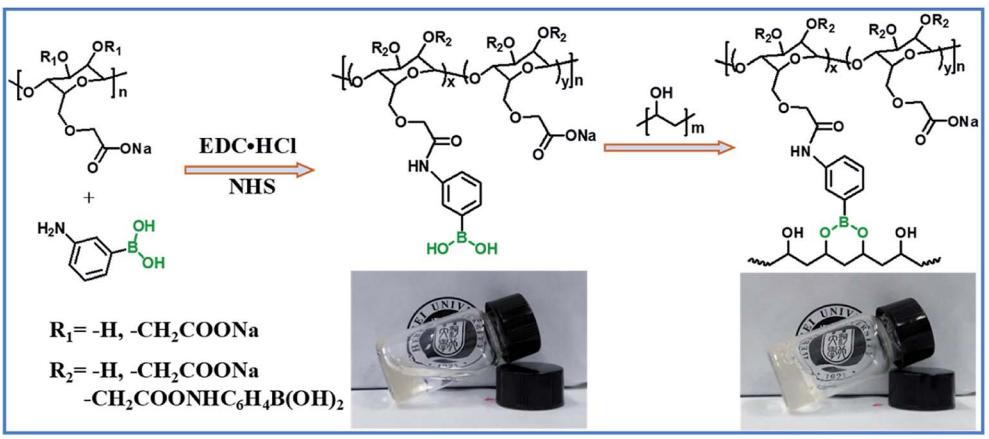

Scheme 1 Synthesis of CMC–B(OH)$_2$ and preparation of the hydrogel.

hydrogel (2%) are inserted for comparison. It was very interesting that the hydrogels could be prepared with very low concentration of gelators, and as a result, the water content in the hydrogel was up to 98–99%. The fast gelation reaction indicated the coupling reaction of phenylboronic acid and 1,3-diols was pretty fast, while the gelation without stimulus ensured biosafety and persistent self-healing property in potential bioapplication. At the same time, there were excess 1,3-diols on PVA, which could endow the hydrogel with fast self-healing property. Based on above procedures, a series of hydrogels with various weight ratio and gelator concentrations were prepared.

The morphology of the hydrogels with very low gelator concentration was observed under a field emission scanning electric microscope (SEM). The SEM images of the hydrogel with 2% are shown in Fig. 2. Although the CMC–$B(OH)_2$ weight ratio in the 2/1 hydrogel was higher than that of PVA, the ratio of hydroxyl group on PVA were still much higher and resulted in regular pore sizes (Fig. 2a). However, the pore size decreased with decreasing of the CMC–$B(OH)_2$ weight ratios. This was due to the higher molecular weight of the CMC–$B(OH)_2$ repeating unit compared to that of PVA. At the same time, because the PVA group was excess in the hydrogels, the cross-linking networks became less compact and size of micropores became less regular (Fig. 2b and c). The interconnected micropores are mutually penetrated with very high ratio of water (98%), which could have good permeability for controlled drugs release, cell culture and nutrients delivery. The hydrogel was also subjected to TGA analysis, the hydrogel with 1/1 ratio exhibits a degradation profile almost followed that of CMC–$B(OH)_2$, which also proved the formation of boronic ester bonds with PVA (Fig. S2†).

Rheology study of the CMC based hydrogels with boronic ester cross-linking

The mechanical property of the hydrogels was determined by rheology study after incubated for 12 h to reach the equilibrium state. The frequency scan of the hydrogels with various weight ratios of CMC–$B(OH)_2$/PVA are shown in Fig. 3. The hydrogels showed solid characteristic of rheology curves with $G' > G''$ within frequency range from 0.1 rad s^{-1} to 100 rad s^{-1}.

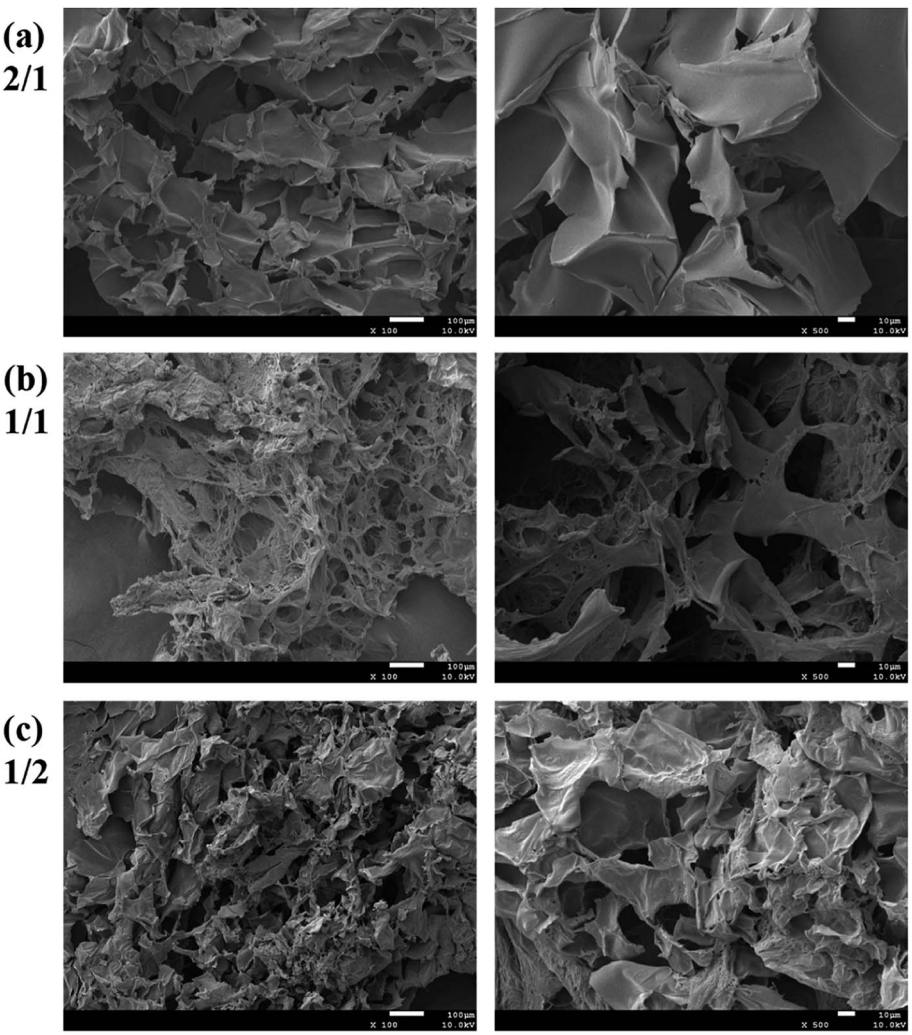

Fig. 2 SEM images of the 2% hydrogel with various CMC–$B(OH)_2$/PVA weight ratios of (a) 2/1, (b) 1/1 and (c) 1/2 (left: 100×; right: 500×).

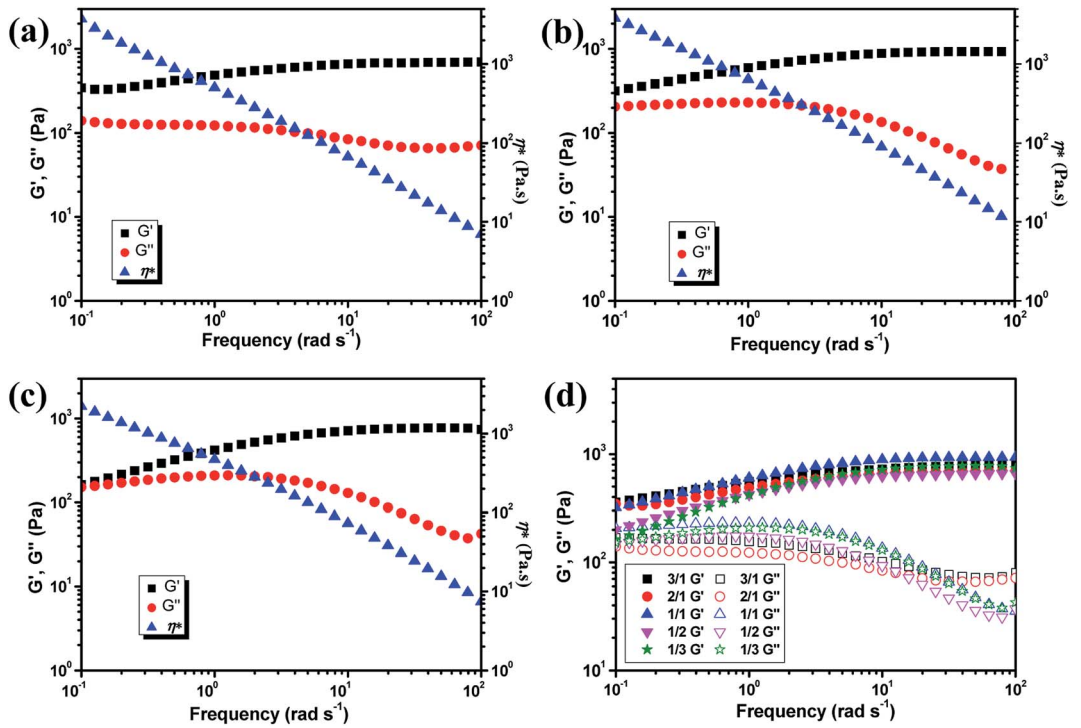

Fig. 3 Rheology curves of the hydrogel with (a) 3/1, (b) 1/1, (c) 1/3 weight ratio of CMC–$B(OH)_2$/PVA and (d) comparison of the modulus of the hydrogels.

Although the gelator concentration was pretty low as 2%, the G' of the hydrogels were pretty high indicated good mechanical strength.[47] However, with decreasing CMC–$B(OH)_2$ ratios, the G' decreased gradually at low frequency range; as a result, the G'' became comparable to G' at 0.1 rad s^{-1} when the weight ratio of CMC–$B(OH)_2$/PVA decreased to 1/3, as shown in Fig. 3a–c. Because of lower molecular weight of PVA repeating unit, the hydroxyl groups were excess and boronic acid could be consumed completely, as a result, higher CMC–$B(OH)_2$ ratio in the hydrogel resulted a higher cross-linking density and less reversible characteristic. The G' and G'' of a series of hydrogels with CMC–$B(OH)_2$/PVA from 3/1 to 1/3 are compared in Fig. 3d. The reversible characteristic of the boronic ester containing hydrogel was possibly through fast substitution of boronic ester group by adjacent hydroxyl groups (Scheme 2). As a result, boronic ester containing hydrogels always illustrate fast reversible characteristic.[37,47] It was observed although the reversible characteristic at low frequency are different, the G' above 1 rad s^{-1} became comparable no matter the compositions, proved the compositions have very important influence on mechanical property of the hydrogel although the CMC–$B(OH)_2$ itself could not form hydrogel at comparable concentration.

The hydrogels also formed with the gelator concentration decreased to 1%, as shown in Fig. 4. The G' decreased with decreasing gelator concentration, but the rheology curves still showed solid characteristic as shown in Fig. 4a. Although low mechanical strength could limit their application property, the hydrogel prepared with extremely low gelator concentration of 1% was still very interesting. The strain scan of the hydrogels was also performed to investigate the flexibility of the hydrogels with various ratios and gelator concentrations. The critical strain of 2% hydrogel with 1/1 composition was about 360% and the G' began to decrease at 205% strain. When the gelator concentration decreased to 1%, the critical strain increased to 380% and the G' began to decrease at 290% strain (Fig. 4b). Other hydrogels also showed the critical strain above 200% (Fig. S3†). As a result, the hydrogel could be subjected to bending and knotting without worrying about breakage, and

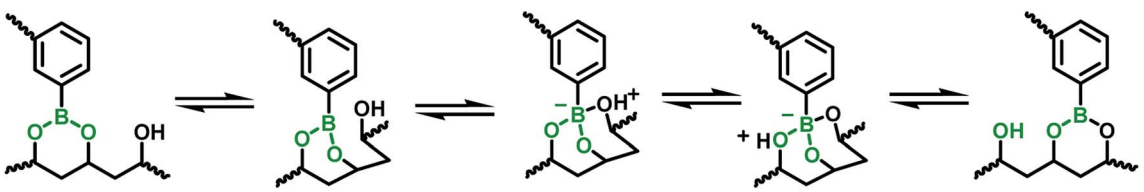

Scheme 2 The mechanism of fast boronic ester exchange through adjacent hydroxyl substitution.

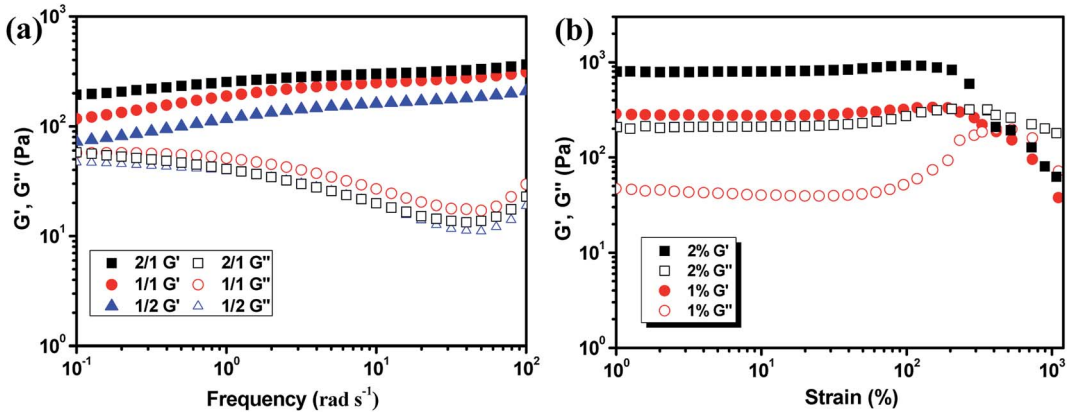

Fig. 4 Rheology curves of the 1% hydrogel with various CMC–$B(OH)_2$/PVA composition (a) and the strain scan of the hydrogels with 1/1 ratio (b).

the elongation could go up to about 350% before breaking (Fig. S4†).

Self-healing of the cellulose based hydrogels with boronic ester cross-linking

The dynamic boronic ester could endow the hydrogel with fast self-healing property based on boronic ester exchange. The self-healing property of the hydrogels in this study was determined with a variety of methods. The hydrogel prepared with 1/1 ratio and 2% concentration was illustrated as an example. The hydrogel samples were stained into different colors and two pieces were contacted together to confirm the self-healing, as shown in Fig. 5. The two hydrogel semicircles merged into one whole hydrogel plate with no scar figured out after 12 h (Fig. 5a and b); however, the different color on each part proved the hydrogel plate was self-healed from two halves. When the self-healed hydrogel was cut again, it can still self-heal within 12 h and could not split under stretching (Fig. 5c and d). The self-healing process was observed under a microscope. When the hydrogel plate was contacted in sealed mold, the hydrogel stride across the gap and began to stick together in 10 min. The different part of the hydrogel attached and the crack smoothed gradually and almost disappeared in 40 min (Fig. 5e–h).

The self-healing property of the hydrogel was also analyzed by rheological tests. The hydrogel plate with 1/1 ratio was operated with alternative amplitude of 1% and 300% above critical strain at 1 rad s^{-1}. When the strain increased from 1% to 300%, the G' decreased from 500 Pa to about 1 Pa, which is lower than G'' and showed the liquid characteristic. When the strain was changed to 1% again, the G' recovered to its initial value, indicating the self-healing of the hydrogel and the recovery of the cross-linked network, as shown in Fig. 6a. This process could be repeated without much difference, proved the self-healing of the CMC–$B(OH)_2$/PVA hydrogen was pretty fast and reversible. The 2% hydrogel with 1/1 weight ratio also

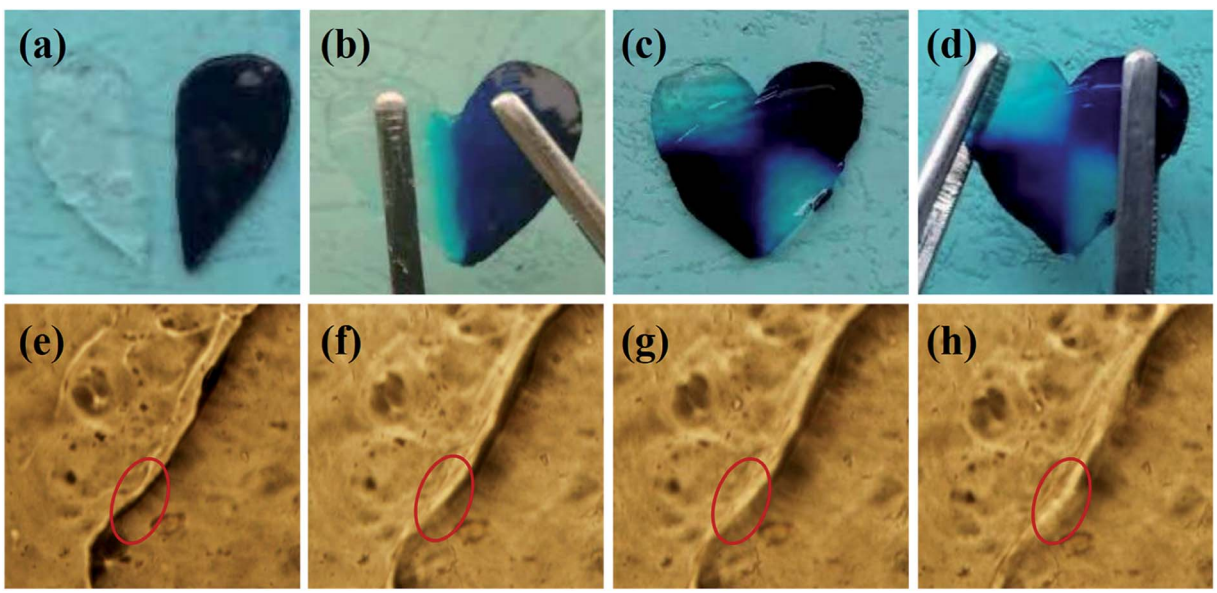

Fig. 5 The self-healing of the hydrogel under bare eyes (a–d) and under microscope ((e) 0 min; (f) 10 min; (g) 20 min; (h) 40 min).

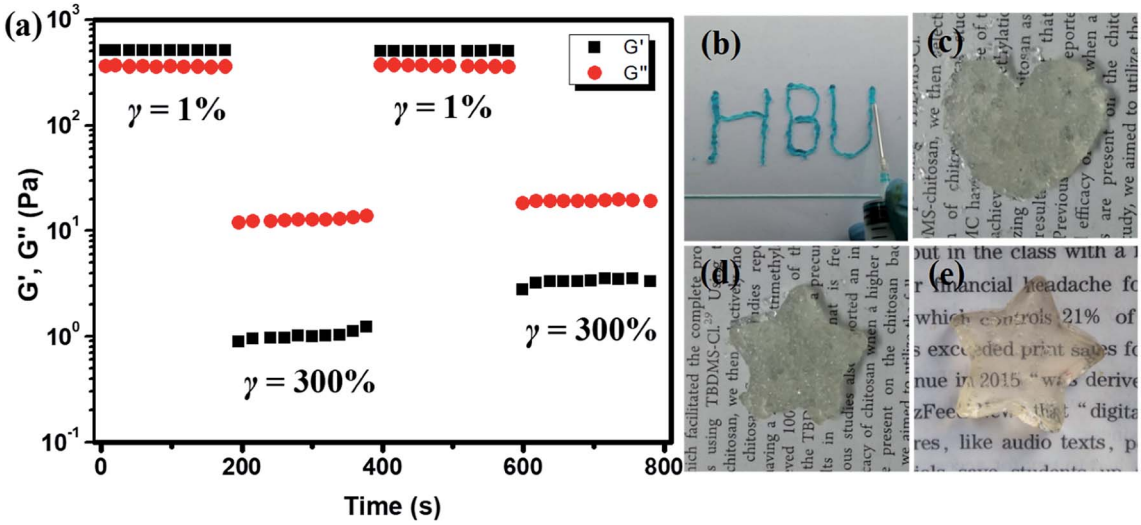

Fig. 6 Multistep amplitude scan of 1 : 1 hydrogel with alternative $\gamma = 1\%$ and $\gamma = 300\%$ (a), injection of the hydrogen through 10# needle (b), the injected shaped hydrogel for 10 min (c and d) and after 12 h (e).

showed injectable property. The hydrogel could be injected through a 10# needle gradually into characters (Fig. 6b). When the hydrogel was injected into molds with various shapes, the hydrogel particles stuck together to form whole hydrogel plates and could hold their own weight within 10 min (Fig. 6c, d and S5†). However, due to the presence of air bubbles, the hydrogel plates were not transparent and the surfaces were not smooth, and the hydrogel plated reassembled into clear hydrogel plate in 12 h (Fig. 6e).

The tensile test of the hydrogel was also carried out to evaluated self-healing efficient (HE) quantitatively. The stress–strain curves of the 2% hydrogel with 1/1 weight ratio are shown in Fig. 7. The original hydrogel showed tensile strength of 11.8 kPa with 384% elongation. At the same time, the self-healed hydrogel also showed good tensile strength with high elongation. The tensile strength of the self-healed hydrogel was 11.6 kPa, comparable to original hydrogel, while the elongation decreased to about 300%. The mechanical strength of the self-healed hydrogel was almost comparable (>95%) to original hydrogel proved the high self-healing efficiency and the decrease of elongation was possibly due to dehydration in previous experiment since the tensile modulus increased a little bit. The optical images of the hydrogel on tensile tester before stretching and at high elongation are inserted in the Fig. 7. Other hydrogels also showed high elongation and good healing efficiency, however, the hydrogels stayed at elongated state after the tensile force was unloaded (Fig. S5†). Previous reports showed the boronic ester bond is pH responsive and the hydrogel could be degraded under acid;[34,45] however, the hydrogels in this research did not show gel–sol–gel transition. When the acid was added onto the hydrogel, phase separation was observed because of protonation of the carboxyl groups since only part of the carboxyl groups were consumed during coupling reaction (Fig. S6†).

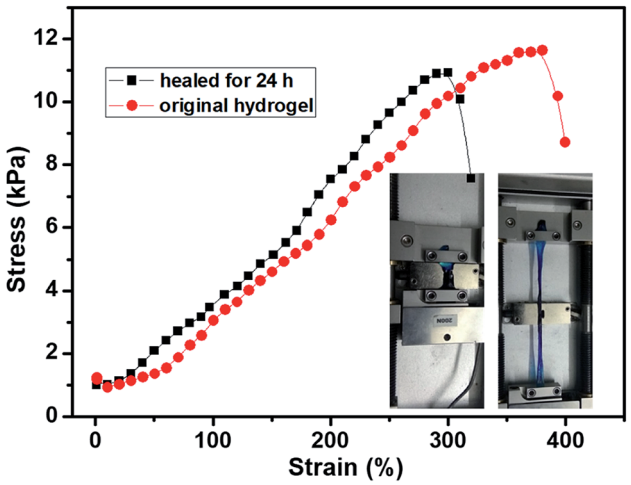

Fig. 7 The tensile curves of the 1/1 hydrogel before and after self-healing (1 mm s^{-1}).

Controlled DOX·HCl release and biocompatibility of the CMC based hydrogel

The application of the hydrogel as drug delivery vehicles were investigated with DOX·HCl as the model anti-cancer drug. The release profiles of the 2% hydrogel with 1/1 ratio in various pH buffers are shown in Fig. 8a. Because of loose cross-linked structure and regular network based on low gelator concentration, the hydrogels showed fast release in first 2 hours. After 2 hours, the drug release rate decreased and became stable with a controlled manner. Then the cumulative DOX·HCl release ratios became almost stable, but not all the drug was released up to 72 h. In pH 7.4 buffer, the hydrogel showed controlled DOX·HCl release from 2 h to 12 h and then reached the plateau gradually to total release ratio of about 40% (Fig. 8a, black line). When the pH of the buffer decreased to 6.5 and 5.4, the DOX·HCl release ratio reached to 55% and 60% respectively at

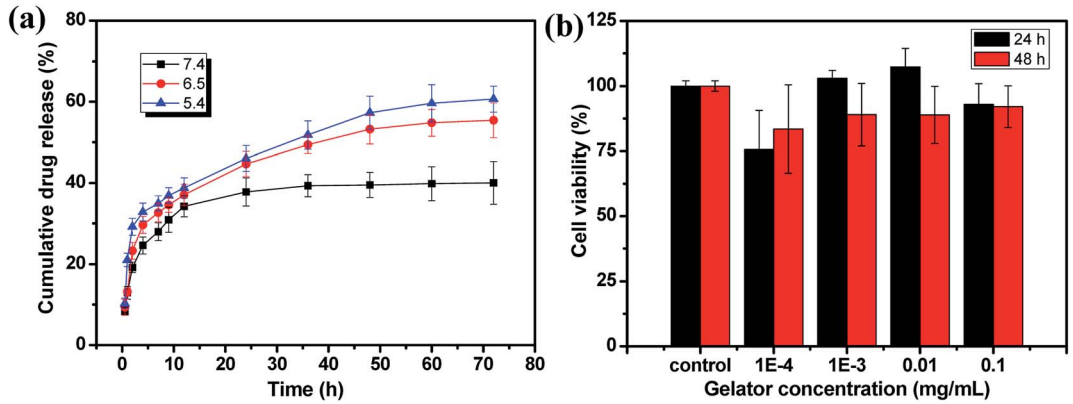

Fig. 8 DOX·HCl release curves (a) and biotoxicity result (b) of the 1 : 1 hydrogel.

72 h (Fig. 8a, red and blue line). With very low gelator concentration, the cross-linking density should be pretty low with larger pore size and the drug release rate should be accelerated. The possible reason for low release rate in pH 7.4 buffer was the hydrophobic property of DOX at physiological condition. As a result, large part of DOX aggregated in the hydrophobic domain of 6-numbered rings on the CMC backbone and only free DOX in the network released to the buffer. However, with decreasing of pH, the DOX protonized gradually and became more hydrophilic, and then defused into the release buffer slowly. This kind of pH sensitive DOX·HCl release could be very useful in potential cancer therapy because the lower pH caused by high metabolization rate at cancer positions.[48,49]

The biocompatibility of hydrogel is a necessary prerequisite for its potential bioapplication as drug loading and delivery vehicle, tissue repairing and wound dressing materials. The biotoxicity of the hydrogel was measured by the CCK-8 assay and the results are shown in Fig. 8b. The hydrogel (1/1) diluents were not toxic to CT-26 cells with viability higher than 75% up to 48 h and other components showed similar results. This result proved the hydrogels prepared from CMC–$B(OH)_2$ and PVA are biocompatible and could be used in potential bioapplications.

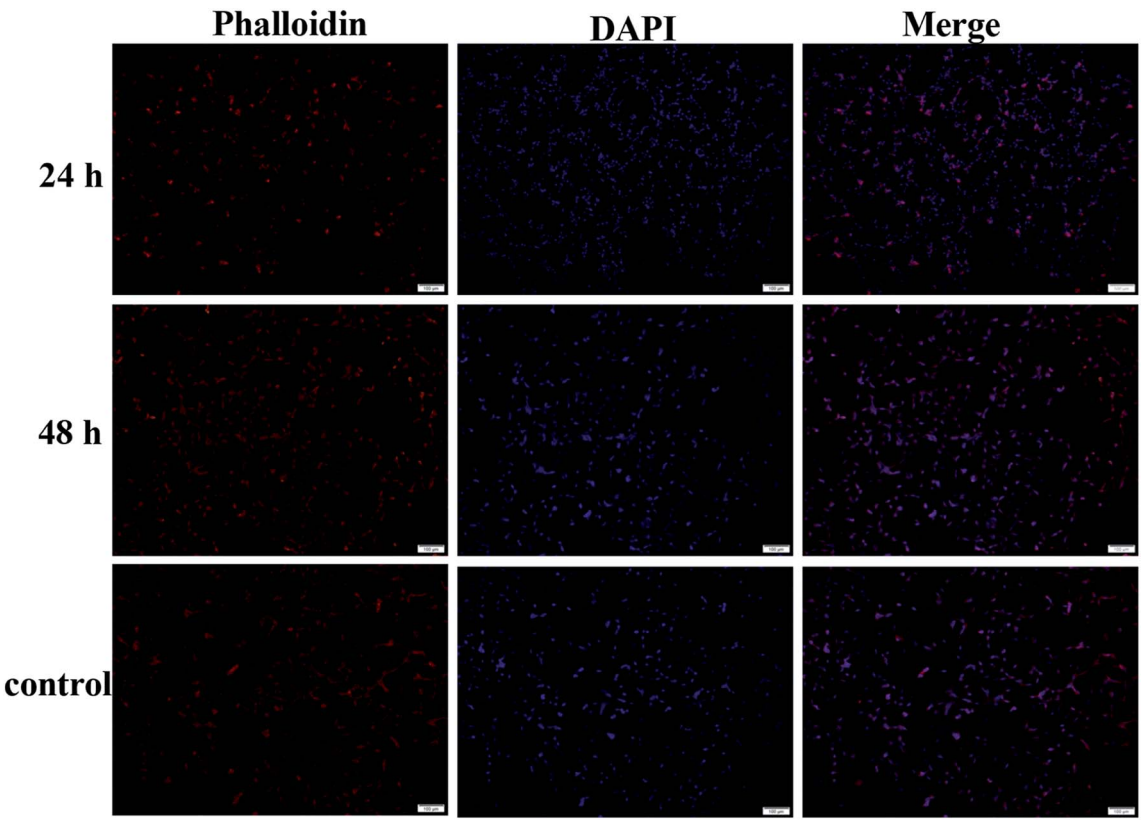

Fig. 9 Fluorescence images of the cells in 0.2% hydrogel (1 : 1) solution at different time.

The cultivation of the cells in hydrogel solution was also carried out to investigate the biocompatibility at high concentration of 0.2%. After cultivated for 24 and 48 h, the cells were stained and observed on a fluorescence microscope, as shown in Fig. 9. The red cytoplasm and blue nucleus are well dispersed in the hydrogel solutions; importantly, the cytoplasm and nucleus could overlap together proved they are derived from the living cells. Moreover, the cell density increased from 24 h to 48 h and the cell density was not lower than that in of the control group, which indicated the cells well proliferated during that period in the hydrogel solution. The hydrogel plates were also immersed in the cell culture medium to investigate the toxicity of hydrogel extract and showed the same results. All above results proved the hydrogels have excellent biocompatibility and could be potentially used in bioscience and technology. As a potential wound dressing material, the flexible self-healing hydrogel can be fitted onto the wound and attached tightly on the skin to provide a closed environment, and then accelerate the wound repairing process.[50] This CMC–$B(OH)_2$/PVA hydrogel could be attached onto the back of the hand and would not fell off when moving the fingers. When the hydrogel was removed from the skin with tweezers, no any hydrogel particle was left proved the moderate adhesion strength of the hydrogel to human skin (Fig. S7†). This feature is also very useful for wound healing because the drug loaded hydrogel need to be replaced regularly during the wound repairing process,[44] which is under investigation.

Conductivity of the CMC based hydrogel

Since large amount of carboxyl groups were ionized in the hydrogel at neutral conditions (Scheme 1), the ionic hydrogel also showed conductivity.[51,52] A circuit was connected with a light-emitting diode (LED) bulb to examine the conductivity of the 1/1 hydrogel. As illustrated in Fig. 10a, the LED lit up when the circuit was connected *via* the hydrogel bar, compared to the water tank. The LED extinguished when the hydrogel was cut in the middle, and the self-healed hydrogel bar also connected the circuit and the LED lit up again after the two hydrogel parts were attached for 1 h (Fig. 10b). The relit of the LED also demonstrated the fast and effective self-healing of the hydrogels.

The conductivity of the ionic hydrogels was investigated to determine the influence of the composition on conductivity of the hydrogels. The electrochemical impedance spectroscopy was performed to measure the conductivity of the hydrogels

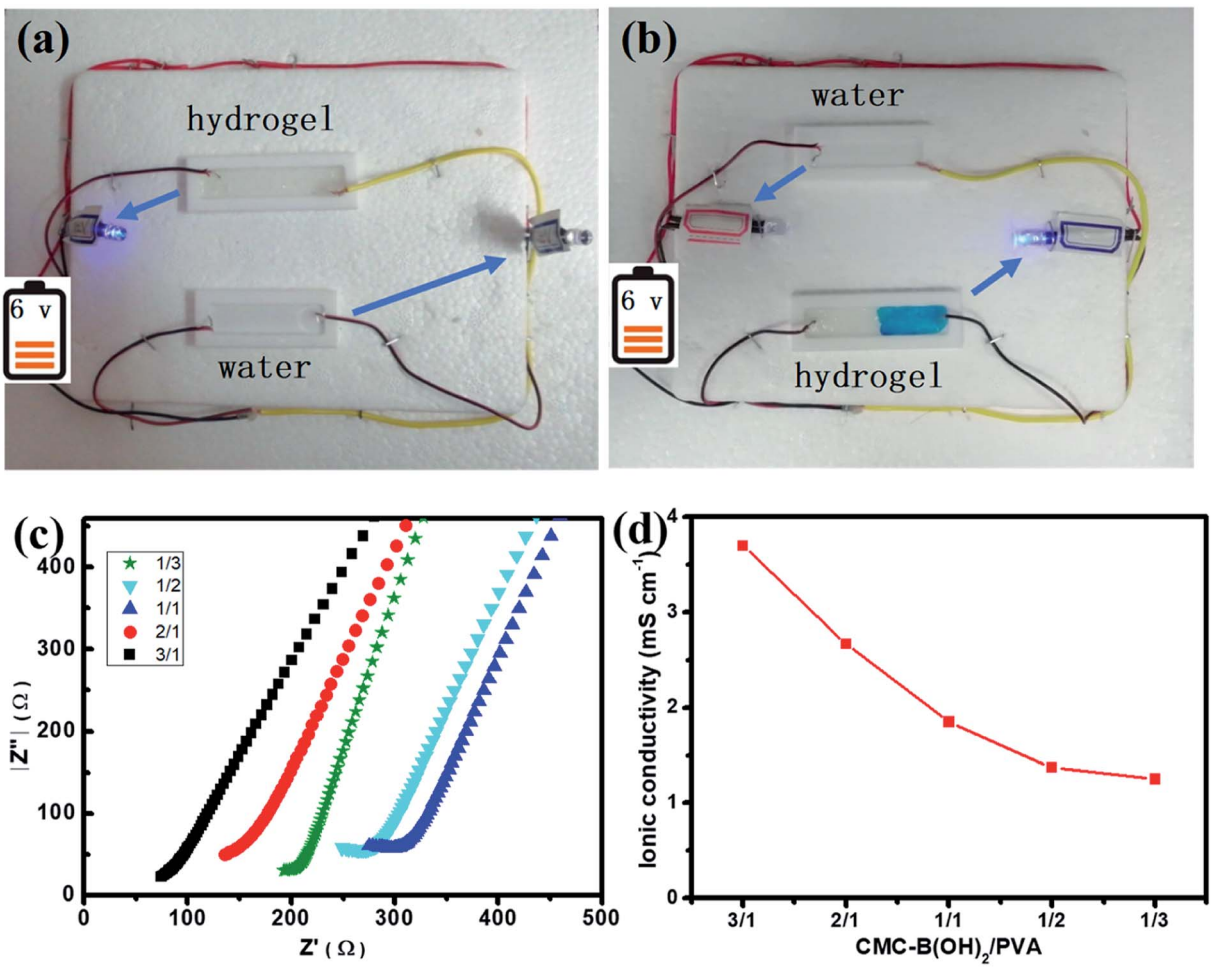

Fig. 10 The conductive property of the as prepared 1/1 hydrogel (a) and self-healed hydrogel (b), the electric resistance (c) and the dependence of ionic conductivity on composition of the hydrogels (d).

quantitatively, as shown in Fig. 10c. Hydrogels with all compositions showed conductive property and the increasing of interfacial resistance indicated the decrease of conductivity. At the same time, the conductivity of the hydrogel decreased with increasing PVA ratios, the conductivity of hydrogels decreased from 3.97 mS cm^{-1} to 1.25 mS cm^{-1} when the CMC–$B(OH)_2$ composition decreased from 3/1 to 1/3 (Fig. 10d). This result proved the conductivity of the hydrogels were originated from the ionized carboxyl groups on CMC–$B(OH)_2$, this property also indicated the conductive hydrogels could be prepared from a series of biobased polymers like sodium alginate, hyaluronic acid, *etc.* and this kind of hydrogels could be used as real-time biosensors in tissue repairing, wound healing processes.[51]

4. Conclusion

Self-healing hydrogels were fabricated from phenylboronic acid functionalized CMC through dynamic boronic ester bond. The phenylboronic acid groups were coupled onto the CMC through coupling reaction and verified by a series of characterizations. The hydrogel with very low gelator concentrations was prepared by reaction of CMC–$B(OH)_2$ and PVA without additional stimulus. Based on biobased CMC, the hydrogel showed excellent biocompatibility and controlled drug release behavior. The hydrogel also showed good mechanical property and conductivity that could be used in biotechnology for real real-time detection. All these properties make the CMC–$B(OH)_2$ based self-healing hydrogels very useful in a series of areas including tissue engineering, wound repairing and controlled drug release.

Conflicts of interest

There are no conflicts to declare.

Acknowledgements

This research was kindly supported by National Natural Science Foundation of China (No. 21374028, 81502477); the Project for Talent Engineering of Hebei Province (No. A2016015001), Natural Science Foundation of Hebei Province (B2018201140, H2019201084).

References

1 S. Azevedo, A. M. S. Costa, A. Andersen, I. S. Choi, H. Birkedal and J. F. Mano, *Adv. Mater.*, 2017, **29**, 1700759.
2 T. C. Tseng, L. Tao, F. Y. Hsieh, Y. Wei, I. M. Chiu and S. H. Hsu, *Adv. Mater.*, 2015, **27**, 3518.
3 M. Kohei, N. Masaki, T. Yoshinori and H. Akira, *Angew. Chem., Int. Ed.*, 2015, **54**, 8984–8987.
4 G. Li, J. Wu, B. Wang, S. Yan, K. Zhang, J. Ding and J. Yin, *Biomacromolecules*, 2015, **16**, 3508–3518.
5 Y. Zhang, L. Tao, S. Li and Y. Wei, *Biomacromolecules*, 2011, **12**, 2894–2901.
6 Y. Guan and Y. Zhang, *Chem. Soc. Rev.*, 2013, **42**, 8106.
7 Z. Wei, J. H. Yang, J. Zhou, F. Xu, M. Zrinyi, P. H. Dussault, Y. Osada and Y. M. Chen, *Chem. Soc. Rev.*, 2014, **43**, 8114–8131.
8 Q. Yang, P. Wang, C. Zhao, W. Wang, J. Yang and Q. Liu, *Macromol. Rapid Commun.*, 2017, **38**, 1600741.
9 Y. Liu and S.-h. Hsu, *Front. Chem.*, 2018, **6**, 449.
10 D. L. Taylor and M. in het Panhuis, *Adv. Mater.*, 2016, **28**, 9060–9093.
11 T. Kakuta, Y. Takashima, M. Nakahata, M. Otsubo, H. Yamaguchi and A. Harada, *Adv. Mater.*, 2013, **25**, 2758.
12 M. Zhang, D. Xu, X. Yan, J. Chen, S. Dong, B. Zheng and F. Huang, *Angew. Chem., Int. Ed.*, 2012, **124**, 7117–7121.
13 T. Cai, S. Huo, T. Wang, W. Sun and Z. Tong, *Carbohydr. Polym.*, 2018, **193**, 54–61.
14 Y.-G. Jia, M. Zhang and X. X. Zhu, *Macromolecules*, 2017, **50**, 9696–9701.
15 Z. Wang, Y. Ren, Y. Zhu, L. Hao, Y. Chen, G. An, H. Wu, X. Shi and C. Mao, *Angew. Chem., Int. Ed.*, 2018, **57**, 9008–9012.
16 A. Phadke, C. Zhang, B. Arman, C.-C. Hsu, R. A. Mashelkar, A. K. Lele, M. J. Tauber, G. Arya and S. Varghese, *Proc. Natl. Acad. Sci. U. S. A.*, 2012, **109**, 4383–4388.
17 X. He, L. Liu, H. Han, W. Shi, W. Yang and X. Lu, *Macromolecules*, 2019, **52**, 72–80.
18 F. Luo, T. L. Sun, T. Nakajima, T. Kurokawa, Y. Zhao, K. Sato, A. B. Ihsan, X. Li, H. Guo and J. P. Gong, *Adv. Mater.*, 2015, **27**, 2722–2727.
19 R. Tian, X. Qiu, P. Yuan, K. Lei, L. Wang, Y. Bai, S. Liu and X. Chen, *ACS Appl. Mater. Interfaces*, 2018, **10**, 17018–17027.
20 T. Yuan, X. Cui, X. Liu, X. Qu and J. Sun, *Macromolecules*, 2019, **52**, 3141–3149.
21 Z. Lei and P. Wu, *ACS Nano*, 2018, **12**, 12860–12868.
22 W. Yang, X. Tao, T. Zhao, L. Weng, E. Kang and L. Wang, *Polym. Chem.*, 2015, **2015**, 7027–7035.
23 S. Mukherjee, M. R. Hill and B. S. Sumerlin, *Soft Matter*, 2015, **11**, 6152–6161.
24 Y. Zhang, C. Fu, Y. Li, K. Wang, X. Wang, Y. Wei and L. Tao, *Polym. Chem.*, 2017, **8**, 537–544.
25 F.-Y. Hsieh, L. Tao, Y. Wei and S.-h. Hsu, *NPG Asia Mater.*, 2017, **9**, e363.
26 R. Dong, X. Zhao, B. Guo and P. X. Ma, *ACS Appl. Mater. Interfaces*, 2016, **8**, 17138–17150.
27 G. H. Deng, F. Y. Li, H. X. Yu, F. Y. Liu, C. Y. Liu, W. X. Sun, H. F. Jiang and Y. M. Chen, *ACS Macro Lett.*, 2012, **1**, 275–279.
28 X. Yang, G. Liu, L. Peng, J. Guo, L. Tao, J. Yuan, C. Chang, Y. Wei and L. Zhang, *Adv. Funct. Mater.*, 2017, **27**, 1703174.
29 P. Wang, G. Deng, L. Zhou, Z. Li and Y. Chen, *ACS Macro Lett.*, 2017, **6**, 881–886.
30 X. Yu, L. Shi and S. Ke, *Bioorg. Med. Chem. Lett.*, 2015, **25**, 5772–5776.
31 R. Chang, X. Wang, X. Li, H. An and J. Qin, *ACS Appl. Mater. Interfaces*, 2016, **8**, 25544–25551.
32 C. C. Deng, W. L. A. Brooks, K. A. Abboud and B. S. Sumerlin, *ACS Macro Lett.*, 2015, **4**, 220–224.
33 R. W. Guo, Q. Su, J. W. Zhang, A. J. Dong, C. G. Lin and J. H. Zhang, *Biomacromolecules*, 2017, **18**, 1356–1364.

34 A. Pettignano, S. Grijalvo, M. Haring, R. Eritja, N. Tanchoux, F. Quignard and D. Diaz Diaz, *Chem. Commun.*, 2017, **53**, 3350–3353.
35 O. R. Cromwell, J. Chung and Z. Guan, *J. Am. Chem. Soc.*, 2015, **137**, 6492–6495.
36 J. J. Cash, T. Kubo, A. P. Bapat and B. S. Sumerlin, *Macromolecules*, 2015, **48**, 2098–2106.
37 A. J. R. Amaral, M. Emamzadeh and G. Pasparakis, *Polym. Chem.*, 2018, **9**, 525–537.
38 H. Huang, X. Wang, J. Yu, Y. Chen, H. Ji, Y. Zhang, F. Rehfeldt, Y. Wang and K. Zhang, *ACS Nano*, 2019, **13**, 3867–3874.
39 C. Wang, M. Fadeev, J. Zhang, M. Vázquez-González, G. Davidson-Rozenfeld, T. He and I. Willner, *Chem. Sci.*, 2018, **9**, 7145–7152.
40 C. Shao, L. Meng, M. Wang, C. Cui, B. Wang, C.-R. Han, F. Xu and J. Yang, *ACS Appl. Mater. Interfaces*, 2019, **11**, 5885–5895.
41 Z. Wei, J. H. Yang, Z. Q. Liu, F. Xu, J. X. Zhou, M. Zrínyi, Y. Osada and Y. M. Chen, *Adv. Funct. Mater.*, 2015, **25**, 1352–1359.
42 H. Tan, C. R. Chu, K. A. Payne and K. G. Marra, *Biomaterials*, 2009, **30**, 2499–2506.
43 R. Zhang, Z. Huang, M. Xue, J. Yang and T. Tan, *Carbohydr. Polym.*, 2011, **85**, 717–725.
44 W. Huang, Y. Wang, Z. Huang, X. Wang, L. Chen, Y. Zhang and L. Zhang, *ACS Appl. Mater. Interfaces*, 2018, **10**, 41076–41088.
45 B. Lu, F. Lin, X. Jiang, J. Cheng, Q. Lu, J. Song, C. Chen and B. Huang, *ACS Sustainable Chem. Eng.*, 2016, **5**, 948–956.
46 Q. Liu, L. Song, S. Chen, J. Gao, P. Zhao and J. Du, *Biomaterials*, 2017, **114**, 23–33.
47 M. Shan, C. Gong, B. Li and G. Wu, *Polym. Chem.*, 2017, **8**, 2997–3005.
48 J. Liu, Y. Huang, A. Kumar, A. Tan, S. Jin, A. Mozhi and X.-J. Liang, *Biotechnol. Adv.*, 2014, **32**, 693–710.
49 H. Li, R. Wu, J. Zhu, P. Guo, W. Ren, S. Xu and J. Wang, *J. Polym. Sci., Part B: Polym. Phys.*, 2015, **53**, 876–884.
50 H. Chen, J. Cheng, L. Ran, K. Yu, B. Lu, G. Lan, F. Dai and F. Lu, *Carbohydr. Polym.*, 2018, **201**, 522–531.
51 C. Shao, M. Wang, L. Meng, H. Chang, B. Wang, F. Xu, J. Yang and P. Wan, *Chem. Mater.*, 2018, **30**, 3110–3121.
52 R. Tong, G. Chen, D. Pan, H. Qi, R. Li, J. Tian, F. Lu and M. He, *Biomacromolecules*, 2019, **20**, 2096–2104.